

DYNAMIC CHAOS IN RADIOPHYSICS AND ELECTRONICS

Analysis of Chaotic Synchronization of Dynamic Systems with Ill-Determined Phases

A. A. Koronovskii and A. E. Khramov

Received November 5, 2003

Abstract—Synchronization of two chaotic systems with ill-determined phases is analyzed. A new method based on the continuous wavelet transformation is proposed for introducing the phase of a chaotic signal.

Phase locking [1, 2] of dynamic chaotic systems is one of the most important phenomena described by the modern theory of nonlinear oscillations. Phase locking has been experimentally observed in RF oscillators [3], lasers [4, 5], electrochemical oscillators [6], cardiac rhythm [7], gas discharge [8, 9], solar activity [10], etc. (see also reviews [11–14]).

To describe and analyze phase locking, phase $\Phi(t)$ of a chaotic signal is introduced [1, 2, 11–14]. Phase locking is interpreted as locking of the phases of chaotic signals in the case when the amplitudes of these signals remain independent and look chaotic. Phase locking results in the coincidence of the signal frequencies. The frequency of a chaotic signal is defined as the mean rate of the phase variation, $\langle \dot{\Phi}(t) \rangle$.

Currently no universal method yielding correct results for any dynamic system exists for introduction of the phase of a chaotic signal. There are a few methods of introducing the phase that are suitable for “good” systems with relatively simple topologies of chaotic attractors. First, phase Φ of a chaotic signal can be introduced as an angle in a polar coordinate system on the (x, y) plane [15, 16]:

$$\Phi = \arctan \frac{y}{x}. \quad (1)$$

However, in this case, all the trajectories of a chaotic attractor projected on the plane (x, y) must rotate around the origin. Sometimes, the coordinates can be transformed to obtain a projection suitable for introducing the phase [13, 15].

Another method of introducing the phase for a chaotic dynamic system uses an analytic signal [1, 11] represented as

$$\zeta(t) = x(t) + j\tilde{x}(t) = A(t)\exp(j\Phi(t)). \quad (2)$$

Here, function $\tilde{x}(t)$ is the Hilbert transform of time realization $x(t)$:

$$\tilde{x}(t) = \frac{1}{\pi} \text{P.V.} \int_{-\infty}^{+\infty} \frac{x(\tau)}{t-\tau} d\tau. \quad (3)$$

In this expression the notation P.V. refers to the principal value of the integral. Phase $\Phi(t)$ of a chaotic signal $x(t)$ can be determined from expressions (2) and (3).

Finally, the surface of a Poincaré section [1, 11] can be used to determine the phase of a chaotic signal:

$$\Phi(t) = 2\pi \frac{t-t_n}{t_{n+1}-t_n} + 2\pi n, \quad t_n \leq t \leq t_{n+1}, \quad (4)$$

where t_n is the instant when the phase trajectory crosses the surface of the Poincaré cross section for the n th time.

All the aforementioned approaches yield similar correct results in the analysis of “good” systems [15]. At the same time, these methods often lead to incorrect results in the analysis of systems with ill-determined phases (see, for example, [13, 17]). Therefore, phase locking of such systems can be revealed by indirect observations [15, 18] and measurements [19].

In this paper we propose a new method to reveal phase locking of dynamic systems with ill-determined phases. The behavior of such systems can be characterized by a continuous set of phases that can be determined using the continuous wavelet transformation [20, 21] of chaotic temporal realization $x(t)$:

$$W(s, t_0) = \int_{-\infty}^{+\infty} x(t)\psi_{s,t_0}^*(t)dt, \quad (5)$$

where the asterisk denotes complex conjugation and $\psi_{s,t_0}(t)$ is the wavelet function obtained from mother wavelet $\psi_0(t)$,

$$\psi_{s,t_0}(t) = \frac{1}{\sqrt{s}} \psi\left(\frac{t-t_0}{s}\right). \quad (6)$$

Here, time scale s governs the width of wavelet $\psi_{s,t_0}(t)$ and t_0 is the time shift of the wavelet function along the time axis. Note that, in the wavelet analysis, the concept

of time scale is normally used instead of the concept of frequency that is conventional for the Fourier transform.

In this study the Morlet wavelet [22] is used as a mother wavelet:

$$\Psi_0(\eta) = \frac{1}{\sqrt[4]{\pi}} \exp(j\omega_0\eta) \exp\left(\frac{-\eta^2}{2}\right). \quad (7)$$

When the wavelet parameter takes the value $\omega_0 = 2\pi$, time scale s of the wavelet transformation and frequency f of the Fourier transformation satisfy the relationship $s = f$.

The wavelet surface

$$W(s, t_0) = |W(s, t_0)| \exp(j\Phi_s(t_0)) \quad (8)$$

characterizes the behavior of the system on each time scale s at any instant t_0 . Quantity $|W(s, t_0)|$ characterizes the presence and intensity of corresponding time scale s at instant t_0 . Normally, the analysis also involves the instantaneous,

$$E(s, t_0) = |W(s, t_0)|^2 \quad (9)$$

and integral,

$$\langle E(s) \rangle = \int |W(s, t_0)|^2 dt_0 \quad (10)$$

energy distributions over time scales.

Using the wavelet transform, we can determine the phase $\Phi_s(t) = \arg W(s, t)$ for each time scale s . In other words, the behavior of each time scale s can be characterized by corresponding phase $\Phi_s(t)$. The set of phases defined in this way most adequately characterizes the behavior of coupled systems.

Let us consider the behavior of two coupled non-identical chaotic oscillators. If the oscillators under consideration are not phase-locked, their behavior is not synchronized on all time scales s . When some of the time scales of the dynamic systems under consideration become synchronized (e.g., when the coupling parameter is increased), phase locking occurs. The remaining time scales remain unsynchronized. In this mode, phase locking is observed on synchronized time scales s :

$$|\Phi_{s1}(t) - \Phi_{s2}(t)| < \text{const.} \quad (11)$$

Here, $\Phi_{s1,2}(t)$ are the continuous phases of the first and second oscillators and correspond to synchronized time scales s .

The number of synchronized time scales increases with the coupling parameter of coupled dynamic systems. The lag synchronization [16] of the oscillators corresponds to the case when all the time scales s of the two systems under consideration are synchronized.

Indeed, it follows from the condition for the lag synchronization $x_1(t - \tau) \approx x_2(t)$ that $W_1(s, t - \tau) \approx W_2(t, s)$ and, hence, $\Phi_{s1}(t - \tau) \approx \Phi_{s2}(t)$. Evidently, in this case, condition (11) for phase locking is satisfied for all time scales.

A further increase in the coupling parameter [16] leads to a decrease in lag time τ . The oscillators tend toward complete synchronization $x_1(t) \approx x_2(t)$. Consequently, the phase difference $\Phi_{s1}(t) - \Phi_{s2}(t)$ approaches zero for all time scales.

Note, on certain time scales s , phase $\Phi_s(t)$ introduced via the wavelet transformation is nonmonotonic: function $\Phi_s(t)$ either increases or decreases on the average and exhibits local maxima and minima. This is related to the effect of the spectral components corresponding to neighboring time scales. Nevertheless, the nonmonotonic variation of phase $\Phi_s(t)$ with time for certain time scales s does not impede ascertainment of phase locking. Moreover, phase $\Phi(t)$ of a chaotic signal introduced by the conventional methods may also be nonmonotonic (see, for example, [17]).

The proposed approach, in which we introduce the set of phases $\Phi_s(t)$ via the wavelet transformation, can successfully be applied to any dynamic systems (including systems with an ill-determined phase).

As a first example, let us consider the behavior of two coupled nonidentical Rössler systems exhibiting screw chaos (Fig. 1):

$$\begin{aligned} \dot{x}_{1,2} &= -\omega_{1,2}y_{1,2} - z_{1,2} + \varepsilon(x_{2,1} - x_{1,2}), \\ \dot{y}_{1,2} &= \omega_{1,2}x_{1,2} + ay_{1,2} + \varepsilon(y_{2,1} - y_{1,2}), \end{aligned} \quad (12)$$

$$\dot{z}_{1,2} = p + z_{1,2}(x_{1,2} - c),$$

where ε is the coupling parameter, $\omega_1 = 0.98$, and $\omega_2 = 1.03$. In accordance with [19], the following values of the control parameters were chosen: $a = 0.22$, $p = 0.1$, and $c = 8.5$.

Figure 2a illustrates the behavior of two coupled Rössler systems for the case when the coupling parameter is relatively small ($\varepsilon = 0.025$). Power spectra $\langle E(s) \rangle$ of the wavelet transform of the two systems are different. However, time scales s corresponding to the maximum energy are virtually the same. Evidently, in this case, the phase difference $\Phi_{s1}(t) - \Phi_{s2}(t)$ infinitely increases on all time scales (Fig. 2a). This means that there are no mutually synchronized time scales in the systems under consideration. Hence, the systems are not synchronized.

When the coupling parameter increases, the systems become phase-locked (see, for example, [16]). Using indirect measurements, Rosenblum *et al.* demonstrated in [19] that two coupled Rössler systems are phase-locked at the coupling parameter $\varepsilon = 0.05$.

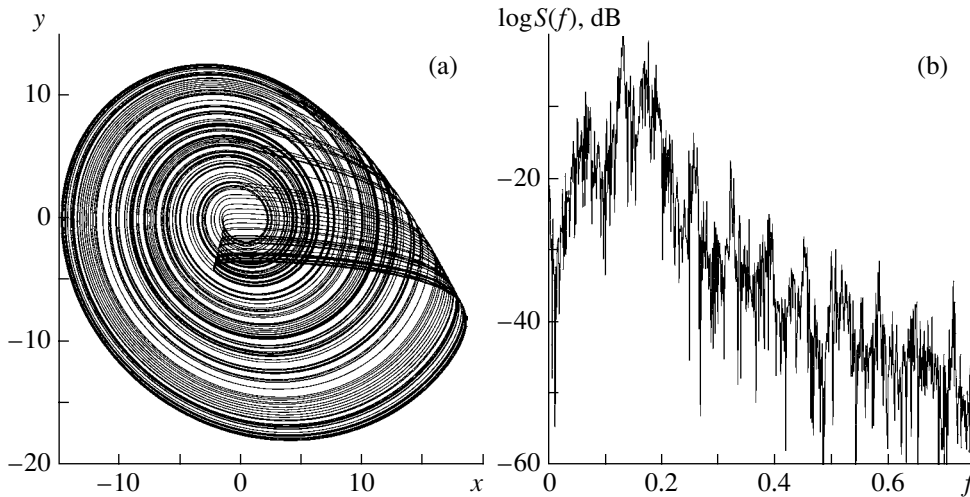


Fig. 1. (a) Projection of the phase portrait on the (x, y) plane and (b) power spectrum for the first Rössler system. The coupling parameter is $\varepsilon = 0$.

Figure 2b shows the behavior of the phase difference $\Phi_{s1}(t) - \Phi_{s2}(t)$ for this case. Phase locking is clearly observed on the time scale $s = 5.25$, which is characterized by maximum energy $\langle E(s) \rangle$ in the wavelet spectrum (Fig. 2b). Thus, it can be concluded that the time scales $s = 5.25$ of the two Rössler systems are mutually synchronized. At the same time, all the time scales adjacent to $s = 5.25$ are also synchronized. Note that strongly differing time scales (e.g., such time scales as $s = 4.5, 6.0$, etc.) remain unsynchronized and phase locking is not observed for these scales (compare Fig. 2b to Fig. 2a). A further increase in the coupling parameter (e.g., to $\varepsilon = 0.07$) results in synchronization of previously unsynchronized time scales (Fig. 2c). It is seen that the time scales $s = 4.5$ are mutually synchronized in contrast to the previous case of $\varepsilon = 0.05$ (Fig. 2b). The number of time scales on which phase locking is observed increases, but, at the same time and as before, some of the time scales (e.g., $s = 3.0$ and 6.0) remain unsynchronized.

When the coupling parameter becomes relatively large (e.g., $\varepsilon = 0.25$), the coupled systems exhibit lag synchronization. In this case the wavelet spectra of the systems coincide (Fig. 2d) and phase locking is observed on all time scales s . Note, when lag synchronization occurs, the phase difference is not zero and depends on lag time τ . As coupling parameter ε increases, the phase difference $\Phi_{s1}(t) - \Phi_{s2}(t)$ (as well as lag time τ) decreases and tends toward zero. Hence, phase locking is transformed into complete synchronization.

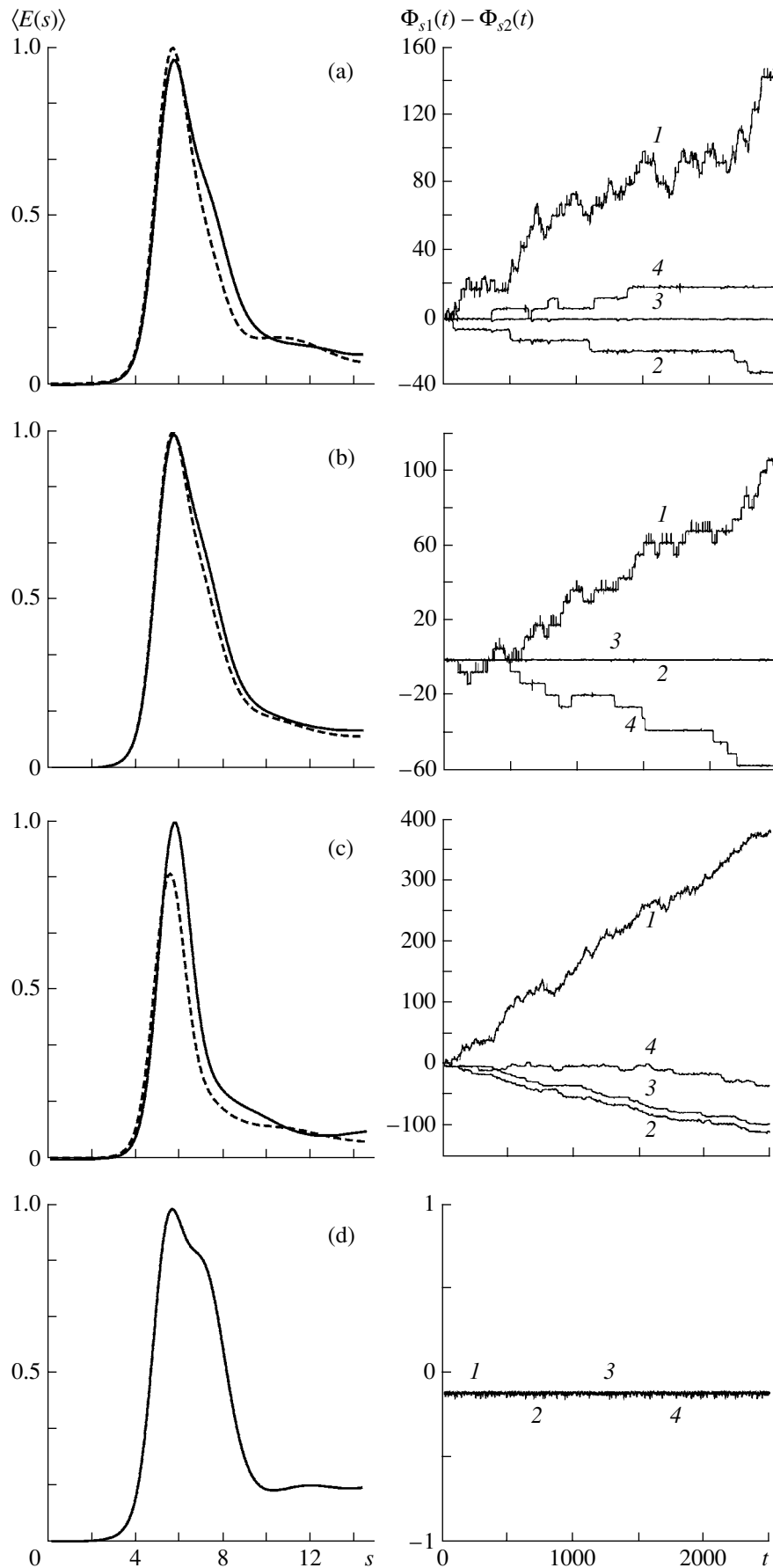
Two coupled RF oscillators with a piecewise-linear characteristic serve as the second example. Such an oscillator, described for the first time in [23] and belonging to the family of Chua circuits, is a simple third-order radio system (Fig. 3). Such a circuit consists of an inductor, capacitors, and a nonlinear element with a piecewise-linear $I-V$ characteristic. An important feature of this system is the presence of two characteristic time scales (two characteristic frequencies). This leads to quasi-periodic oscillations at certain values of the control parameters [24, 25]. In the phase space, the behavior of the system corresponds to a 2D torus; therefore, the system is known as a torus oscillator. In addition, the system may exhibit periodic oscillations (associated with resonant cycles in the phase space) and chaotic oscillations [26, 27].

The coupled oscillators are described by the following dimensionless differential equations:

$$\begin{aligned} \dot{x}_{1,2} &= -\frac{\alpha_{1,2}}{\gamma} f(y_{1,2} - x_{1,2}), \\ \dot{y}_{1,2} &= -\frac{1}{\gamma} (f(y_{1,2} - x_{1,2}) + z_{1,2}) + \frac{\varepsilon}{\gamma} (y_{2,1} - y_{1,2}), \\ \dot{z}_{1,2} &= \gamma y_{1,2}, \end{aligned} \quad (13)$$

where, $x_{1,2} = V_{C_1}^{1,2}/E$ and $y_{1,2} = V_{C_2}^{1,2}/E$ are the dimensionless voltages across the first and second capacitors $C_1^{1,2}$ and C_2 of the first and second oscillator, respectively, and E is the normalization parameter [24, 27].

Fig. 2. (Left panels) Normalized energy spectrum $\langle E(s) \rangle$ of the wavelet transform for (solid line) the first and (dashed line) second Rössler systems and (right panels) the phase difference $\Phi_{s1}(t) - \Phi_{s2}(t)$ for two coupled Rössler systems: (a) $\varepsilon = 0.025$ and synchronization is absent; (b) $\varepsilon = 0.05$, the time scales $s = 5.25$ are mutually synchronized, and the systems are phase-locked; (c) $\varepsilon = 0.07$; and (d) $\varepsilon = 0.25$, all the time scales are synchronized, and the systems are lag-synchronized. For curves 1 in panels (a–d), $s = 3.0$; for curves 2 in panels (a–d), $s = 4.5$; for curves 3 in panels (a–d), $s = 5.25$; for curve 4 in panel (a), $s = 6.5$; and, for curves 4 in panels (b–d), $s = 6.0$.



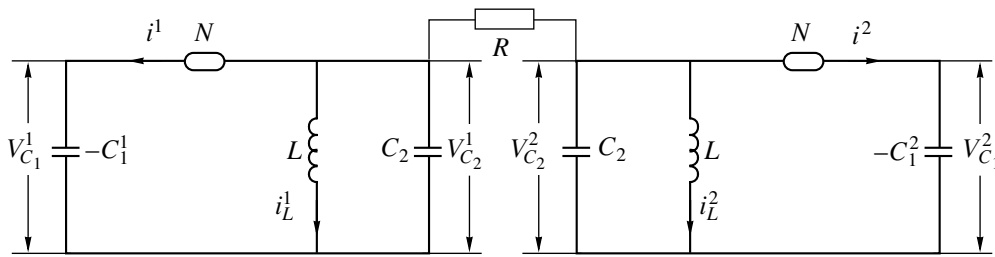


Fig. 3. Two mutually coupled torus oscillators.

The dimensionless parameters are $\alpha_{1,2} = C_2/C_1^{1,2}$ and $\gamma = \frac{1}{m_1} \sqrt{C_2/L}$, and $\tau = t/\sqrt{LC_2}$ is the dimensionless time. Function $f(\xi)$ is the dimensionless $I-V$ characteristic of nonlinear element N determined by the formula

$$f(\xi) = \frac{m_0}{m_1} \xi + \frac{1}{2} \left(\frac{m_0}{m_1} \right) (|\xi + 1| - |\xi - 1|),$$

where m_0 and m_1 are the conductances of the corresponding branches on the piecewise-linear $I-V$ characteristic of element N [24, 27]. The coupling parameter $\varepsilon = 1/Rm_1$ determines the mutual influence of the oscillators under study. In the case of uncoupled systems ($R = \infty$), the coupling parameter is zero.

The following values of the control parameters were chosen: $\alpha_1 = 2.78$, $\alpha_2 = 2.89$, and $\gamma = 3.00$. At these values, both systems exhibit chaotic oscillations in the autonomous regime. Figure 4 demonstrates the projections of the phase portraits and the power spectrum for the first oscillator. A relatively small mismatch of parameters α_1 and α_2 accounts for a slight nonidentity of the subsystems under study.

As was mentioned, a characteristic feature of the oscillator under consideration is the presence of two characteristic time scales (two spectral components $f_a \approx 0.161$ and $f_b \approx 0.032$) that determine the behavior of the system (Fig. 4c). Hence, the wavelet spectra of oscillations exhibit maxima at the corresponding time scales $s_a = 1/f_a \approx 6.2$ and $s_b = 1/f_b \approx 30.0$. In this case the dynamics of self-oscillators can be synchronized at one frequency (on one time scale) and unsynchronized at the other frequency. Phase locking occurring at frequency f_a (Fig. 4c) can easily be revealed by conventional methods since the projection of the chaotic attractor on the (y, z) plane (Fig. 4b) makes it possible to introduce phase $\Phi(t)$ of the chaotic signal (e.g., via expression (1)). This phase is determined by the dynamics of the system at the aforementioned frequency. However, by the conventional approaches, it is impossible to find out if the coupled oscillators are synchronized on the second characteristic time scale, since introduced phase $\Phi(t)$ of the chaotic signal does not depend on the behavior of the system at frequency f_b . In

this context it can be stated that the oscillator under study is a system with an ill-determined phase at the second eigenfrequency of the system. At the same time, the analysis of the dynamics of coupled oscillators based on the set of phases $\Phi_s(t)$ makes it possible to easily find out if the coupled oscillators exhibit synchronous behavior at both frequencies.

Consider the phase difference $\Phi_{s1}(t) - \Phi_{s2}(t)$ on characteristic time scales s at fixed values of the control parameters and various values of coupling parameter ε . As could be expected, in the absence of coupling, the self-oscillators are unsynchronized on all time scales (Fig. 5a). If the coupling parameter is $\varepsilon = 0.05$ and the self-oscillators are phase-locked, the chaotic-signal phases introduced using a conventional approach (e.g., using expression (1)) turn out to be locked. Similar conclusions can be drawn on the basis of the analysis of the time dependence of the phase difference $\Phi_{s1}(t) - \Phi_{s2}(t)$ for the time scale $s_a = 6.2$ (Fig. 5b). At the same time, the phase difference infinitely increases (decreases) on the remaining time scales (including the time scale $s_b = 30.0$). This testifies that these time scales remain unsynchronized. Thus, conventional methods applied to analyze the phases of chaotic signals in coupled systems indicate the presence of phase locking. However, in this case, only one of the two characteristic time scales is synchronized. The second time scale (the second frequency) remains unsynchronized at the aforementioned values of the control parameters and coupling parameter ε .

While the coupling parameter continues to increase, the second characteristic time scale s_b also becomes synchronized (Fig. 5c). Note that the remaining time scales remain unsynchronized. Therefore, the coupled systems under study exhibit phase locking of oscillations but phase locking now takes place for both characteristic time scales. Evidently, in the framework of conventional approaches, the phase-locking regimes illustrated in Figs. 5b and 5c are virtually identical, whereas the proposed method of analysis of the system behavior, which is based on the set of phases $\Phi_s(t)$, enables discrimination between the two cases.

Finally, note a few important aspects. The conventional methods based on expressions (1)–(4) and applied to reveal phase locking involve introduction of

the phase of a chaotic signal and are correct for a temporal series whose Fourier spectrum contains a pronounced component at distinct fundamental frequency f_0 . In this case, phase Φ_{s_0} introduced for the time scale $s_0 \approx 1/f_0$ corresponds to phase $\Phi(t)$ of a chaotic signal introduced by conventional method (1)–(4). Indeed, chaotic-signal phase $\Phi(t)$ is close to phase $\Phi_{s_0}(t)$ of the component at fundamental frequency f_0 (and, hence, on fundamental time scale s_0) since the remaining frequencies (or, which is the same, the remaining time scales) are insignificant in the Fourier spectrum. Evidently, in this case, the mean frequencies $\bar{f} = \langle \dot{\Phi}(t) \rangle$ and $\bar{f}_{s_0} = \langle \dot{\Phi}_{s_0}(t) \rangle$ must be equal to each other and to fundamental frequency f_0 of the Fourier spectrum (see also [17]):

$$\bar{f} = \bar{f}_{s_0} = f_0. \quad (14)$$

Therefore, instantaneous phase $\Phi(t)$ of a chaotic signal can be introduced by the wavelet transformation: $\Phi(t) = \Phi_{s_{\text{fix}}}(t)$. Here, time scale s_{fix} is close to time scale s_0 corresponding to fundamental frequency component f_0 (see, for example, [28]). In particular, it is demonstrated in [29] that, in this case, the wavelet transformation can be interpreted as signal filtering (selection of a certain frequency band in the vicinity of fundamental spectral component f_0) followed by the Hilbert transformation. Apparently, if a time scale lying relatively far from $s_0 = 1/f_0$ is chosen as s_{fix} , the introduced instantaneous phase of a chaotic signal will not allow diagnostics of phase locking even if this effect is discerned in the system under study [29].

If a chaotic time realization is characterized by the Fourier spectrum without a distinct fundamental spectral component (e.g., the spectrum of a Rössler system shown in Fig. 1), the conventional approach based on expressions (1)–(4) can hardly be used because it may yield incorrect results [17]. Evidently, in this case, it is necessary to analyze the behavior of the system on various time scales. This is generally impossible if we use the concept of instantaneous phase $\Phi(t)$ of a chaotic signal introduced by formulas (1)–(4). On the contrary, the proposed approach, which is based on the continuous wavelet transformation and employs a continuous set of phases, can be used to analyze any chaotic signal.

Second, the proposed approach can be used to analyze experimental results since it does not require *a priori* data regarding the system under study. Moreover, in a few cases, the application of the wavelet transformation may reduce the noise effect [21, 30]. It is likely that the method proposed can effectively be used in the analysis of the temporal series generated by physical, biological, physiological, and other systems.

Finally, note that the analysis of the system on all time scales that is based on the continuous wavelet transformation makes it possible to study various types of the behavior of coupled oscillators (complete syn-

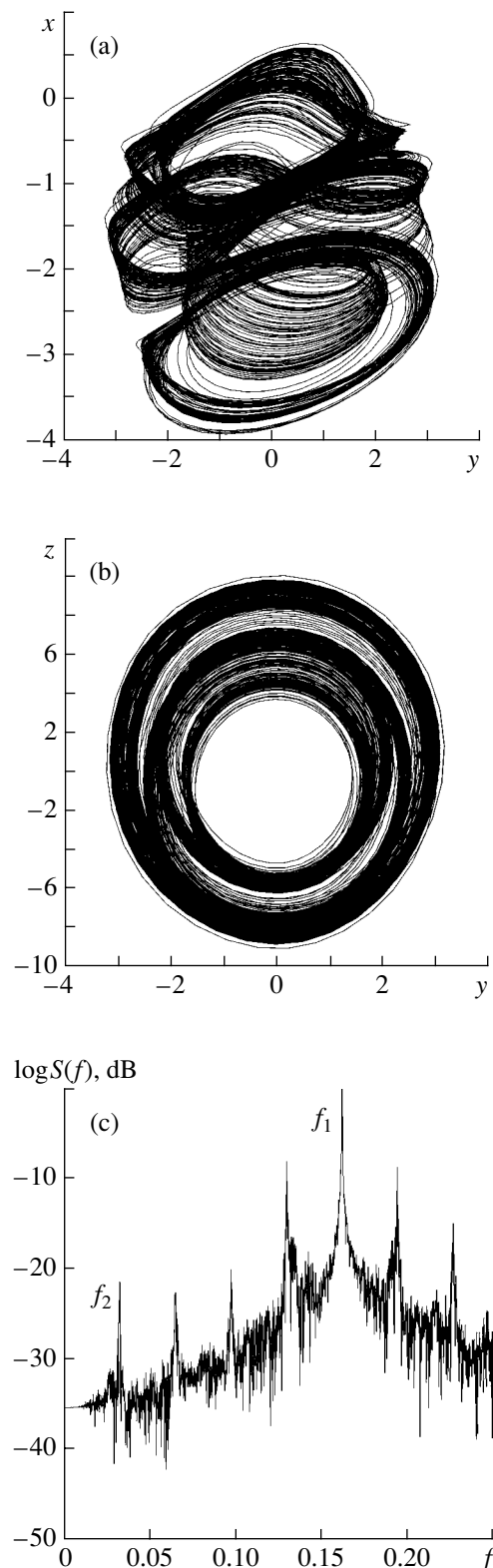


Fig. 4. Projections of the phase portraits on the (a) (y, x) and (b) (y, z) planes for the first torus oscillator (the control parameters are $\alpha_1 = 2.78$ and $\gamma = 3.0$ and the coupling parameter is $\varepsilon = 0$) and (c) spectrum of a chaotic signal calculated using the time realization of the y coordinate at the same values of the control parameters.

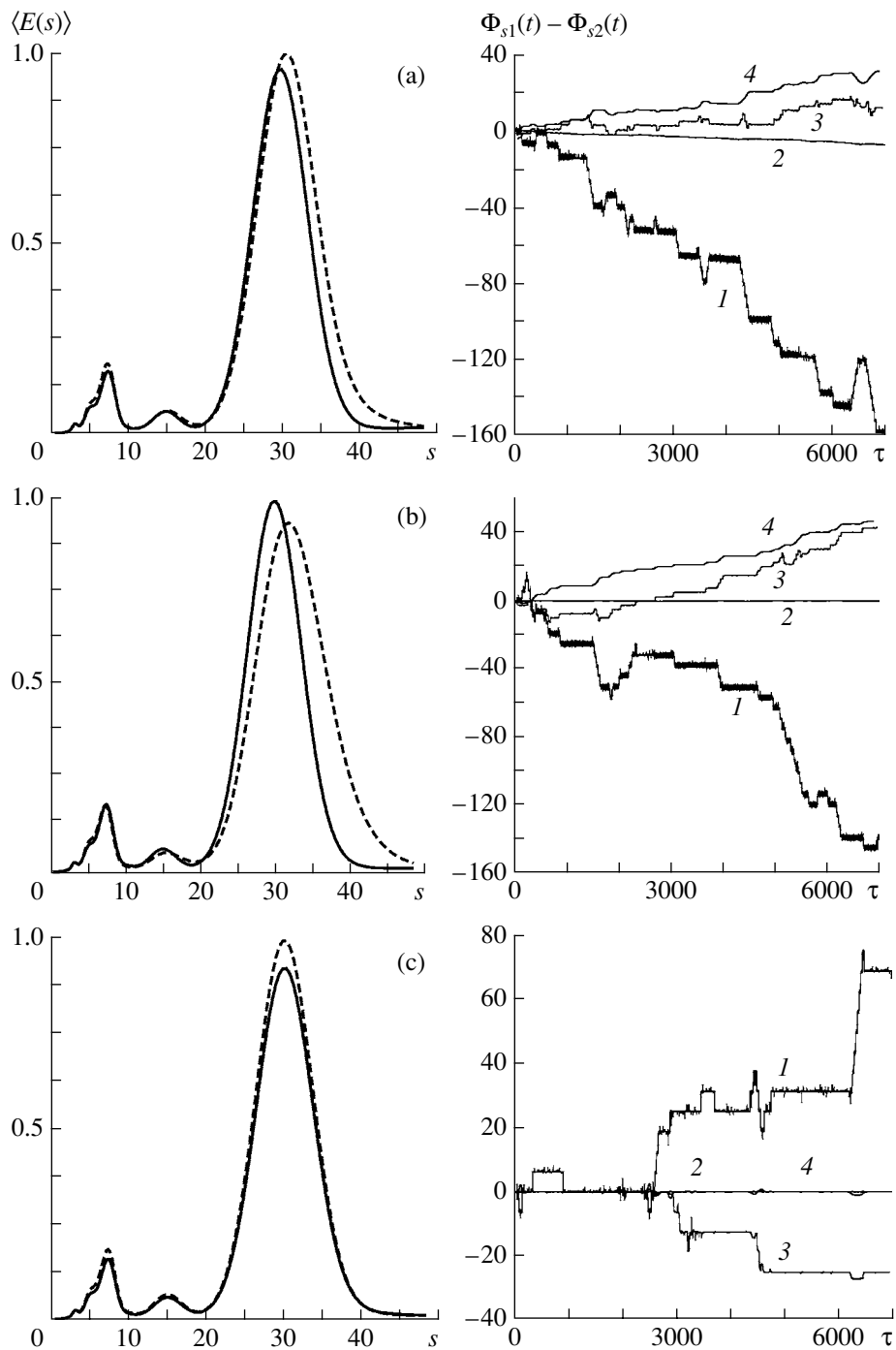


Fig. 5. (Left panels) energy spectra of the wavelet transform of time dependences $x_{1,2}(t)$ for (solid lines) the first and (dashed line) second oscillators and (right panels) the phase difference $\Phi_{s1}(t) - \Phi_{s2}(t)$ for various time scales s of the torus oscillators: $\varepsilon =$ (a) 0, (b) 0.05, and (c) 0.25; $s =$ (1) 4.0, (2) 6.2, (3) 15, and (4) 30.

chronization, lag synchronization, phase locking, and asynchronous oscillations) by a unified approach. Evidently, the number of synchronized time scales uniquely determines the type of behavior. Apparently, it is possible to introduce a quantitative characteristic of the degree of synchronization. Note also that the proposed approach (with minor variations) can be used to

describe the behavior of dynamic systems under an external (e.g., harmonic) action.

Thus, in this study, a new method was proposed for describing phase locking and is based on the continuous wavelet transformation and the analysis of the dynamics of systems on various time scales. This approach can be used to study any dynamic systems

(including dynamic systems with an ill-determined phase) and experimental temporal series.

ACKNOWLEDGMENTS

This study was supported by the Ministry of Education and Science of the Russian Federation (the program Development of the Scientific Potential of Higher Institutes of Learning, project no. 333; the program Leading Scientific Schools, project no. NSh-1250.2003.02; and the program "Universities of Russia," project no. UR.01.01.371), the Russian Foundation for Basic Research (project no. 05-02-16273), Saratov State University (the scientific and educational center "Nonlinear Dynamics and Biophysics"), the Civilian Research and Development Foundation (USA) (grant no. REC-006), the foundation for noncommercial programs "Dynasty," and the International Center for Fundamental Physics.

REFERENCES

1. M. G. Rosenblum, A. S. Pikovsky, and J. Kurths, *Phys. Rev. Lett.* **76**, 1804 (1996).
2. G. V. Osipov, A. S. Pikovsky, and M. G. Rosenblum, *Phys. Rev. E* **55**, 2353 (1997).
3. U. Parlitz, L. Junge, and W. Lauterborn, *Phys. Rev. E* **54**, 2115 (1996).
4. D. Y. Tang, R. Dykstra, M. W. Hamilton, and N. R. Heckenberg, *Phys. Rev. E* **57**, 3649 (1998).
5. E. Allaria, F. T. Arecchi, and A. D. Garbo, *Phys. Rev. Lett.* **86**, 791 (2001).
6. I. Z. Kiss and J. L. Hudson, *Phys. Rev. E* **64**, 046215 (2001).
7. V. S. Anishchenko, A. G. Balanov, N. B. Janson, *et al.*, *Int. J. Bifurcation Chaos* **10**, 2339 (2000).
8. C. M. Ticos, E. Rosa, W. B. Pardo, *et al.*, *Phys. Rev. Lett.* **85**, 2929 (2000).
9. E. Rosa, W. B. Pardo, C. M. Ticos, *et al.*, *Int. J. Bifurcation Chaos* **10**, 2551 (2000).
10. M. Palus, J. Kurths, U. Schwarz, *et al.*, *Int. J. Bifurcation Chaos* **10**, 2519 (2000).
11. A. S. Pikovsky, M. G. Rosenblum, and J. Kurths, *Int. J. Bifurcation Chaos* **10**, 2291 (2000).
12. V. S. Anishchenko and T. E. Vadivasova, *Radiotekh. Elektron. (Moscow)* **47**, 133 (2002) [*J. Commun. Technol. Electron.* **47**, 117 (2002)].
13. A. S. Pikovsky, M. G. Rosenblum, and J. Kurths, *Synchronization: A Universal Concept in Nonlinear Sciences* (Cambridge University Press, Cambridge, 2001).
14. V. S. Anishchenko, V. Astakhov, A. Neiman, *et al.*, *Nonlinear Dynamics of Chaotic and Stochastic Systems. Tutorial and Modern Developments* (Springer Verlag, Heidelberg, 2001).
15. A. S. Pikovsky, M. G. Rosenblum, G. Osipov, *et al.*, *Physica D* **104**, 219 (1997).
16. M. G. Rosenblum, A. S. Pikovsky, and J. Kurths, *Phys. Rev. Lett.* **78**, 4193 (1997).
17. T. E. Vadivasova and V. S. Anishchenko, *Radiotekh. Elektron. (Moscow)* **49**, 76 (2004) [*J. Commun. Technol. Electron.* **49**, 69 (2004)].
18. A. S. Pikovsky, M. G. Rosenblum, and J. Kurths, *Europhysics Lett.* **34**, 165 (1996).
19. M. G. Rosenblum, A. S. Pikovsky, and J. Kurths, *Phys. Rev. Lett.* **89**, 264102 (2002).
20. I. Daubechies, *Ten Lectures on Wavelets* (SIAM, Philadelphia, 1992).
21. A. A. Koronovskii and A. E. Khramov, *Continuous Wavelet Analysis and Its Applications* (Fizmatlit, Moscow, 2003).
22. A. Grossman and J. Morlet, *SIAM J. Math. Anal.* **15**, 273 (1984).
23. T. Matsumoto, L. O. Chua, and R. Tokunaga, *IEEE Trans. Circuits Syst.* **34**, 240 (1987).
24. A. V. Andrushkevich, A. A. Kipchatov, L. V. Krasichkov, *et al.*, *Izv. Vyssh. Uchebn. Zaved., Radiofiz.* **38**, 1195 (1995).
25. A. A. Koronovskii, *Izv. Vyssh. Uchebn. Zaved., Prikladnaya Nelineinaya Dinamika* **5**, 24 (1997).
26. A. A. Kipchatov and A. A. Koronovskii, *Izv. Vyssh. Uchebn. Zaved., Prikl. Nelin. Din.* **5**, 17 (1997).
27. E. N. Egorov and A. A. Koronovskii, *Izv. Vyssh. Uchebn. Zaved., Prikl. Nelin. Din.* **10**, 104 (2002).
28. J. P. Lachaux, E. Rodriguez, and M. van Quyen, *Int. J. Bifurcation Chaos* **10**, 2429 (2000).
29. R. Q. Quiroga, A. Kraskov, T. Kreuz, and P. Grassberg, *Phys. Rev. E* **65**, 041903 (2002).
30. V. A. Gusev, A. A. Koronovskii, and A. E. Khramov, *Pis'ma Zh. Tekh. Fiz.* **29**, 61 (2003) [*Tech. Phys. Lett.* **29**, 775 (2003)].